Stem Cell Reviews and Reports
https://doi.org/10.1007/s12015-020-10062-1

# Multidimensional Proteomic Approach of Endothelial Progenitors Demonstrate Expression of KDR Restricted to CD19 Cells

Coralie L. Guerin[1,2,3] · Léa Guyonnet[1,2,3] · Guillaume Goudot[4] · Dominique Revets[3] · Maria Konstantinou[3] · Anna Chipont[3] · Richard Chocron[5,6] · Adeline Blandinieres[1,7] · Lina Khider[4] · Jeanne Rancic[1,8] · Christophe Peronino[1,7] · Benjamin Debuc[1,9] · Audrey Cras[1,10] · Camille Knosp[5] · Christian Latremouille[1,11] · Antoine Capel[12] · Markus Ollert[3] · Jean-Luc Diehl[1,8,13] · Piet Jansen[12] · Benjamin Planquette[1,8,14] · Olivier Sanchez[1,8,14] · Pascale Gaussem[1,15] · Tristan Mirault[5,16] · Alain Carpentier[1,11] · Nicolas Gendron[1,7] · David M. Smadja[1,7,17]

Accepted: 18 October 2020


## Abstract

Endothelial progenitor cells (EPCs) are involved in vasculogenesis and cardiovascular diseases. However, the phenotype of circulating EPCs remains elusive but they are more often described as $CD34^+KDR^+$. The aim of the study was to extensively characterize circulating potential vasculogenic stem cell candidates in two populations of patients with cardiovascular disease by powerful multidimensional single cell complementary cytometric approaches (mass, imaging and flow). We identified cellular candidates in one patient before and after bioprosthetic total artificial heart implantation and results were confirmed in healthy peripheral and cord blood by mass cytometry. We also quantified cellular candidates in 10 patients with different COVID-19 severity. Both C-TAH implantation and COVID-19 at critical stage induce a redistribution of circulating $CD34^+$ and $CD19^+$ sub-populations in peripheral blood. After C-TAH implantation, circulating $CD34^+$ progenitor cells expressed c-Kit stem marker while specific subsets $CD34^+CD133^{-/+}CD45^{-/dim}$c-$Kit^+KDR^-$ were mobilized. KDR was only expressed by $CD19^+$ B-lymphocytes and $CD14^+$ monocytes subpopulations in circulation. We confirmed by mass cytometry this KDR expression on $CD19^+$ in healthy peripheral and cord blood, also with a VE-cadherin expression, confirming absence of endothelial lineage marker on $CD34^+$ subtypes. In COVID-19, a significant mobilization of $CD34^+$c-$Kit^+KDR^-$ cells was observed between moderate and critical COVID-19 patients regardless CD133 or CD45 expression. In order to better evaluate EPC phenotype, we performed imaging flow cytometry measurements of immature $CD34^+KDR^+$ cells in cord blood and showed that, after elimination of non-circular events, those cells were all $CD19^+$. During COVID-19, a significant mobilization of $CD19^+KDR^+$ per million of $CD45^+$ cells was observed between moderate and critical COVID-19 patients regardless of CD34 expression. $CD34^+$c-$Kit^+$ cells are mobilized in both cardiovascular disease described here. KDR cells in peripheral blood are CD19 positive cells and are not classic vasculogenic stem and/or progenitor cells. A better evaluation of c-Kit and KDR expressing cells will lead to the redefinition of circulating endothelial progenitors.

**Keywords** Stem cells · Endothelial progenitors · C-kit · VEGFR-2/KDR · Bioprosthetic total artificial heart · COVID-19

**Abbreviations**

| | |
|---|---|
| CD | cluster of differentiation |
| COVID-19 | coronavirus disease 2019 |
| EPCs | Endothelial progenitor cells |
| C-TAH | Carmat total artificial heart |
| HSNE | Hierarchical Stochastic Neighbor Embedding |
| SARS-CoV-2 | Coronavirus 2 of Severe Acute Respiratory Syndrome |
| SC | stem cells |

**Supplementary Information** The online version contains supplementary material available at https://doi.org/10.1007/s12015-020-10062-1.

This article belongs to the Topical Collection: *Special Issue on COVID-19 Pandemic and Stem Cells*
Guest Editor: Mariusz Z. Ratajczak

✉ David M. Smadja
david.smadja@aphp.fr

Extended author information available on the last page of the article

Published online: 17 November 2020

| | |
|---|---|
| SPADE | Spanning-tree Progression Analysis of Density-normalized Events |
| UMAP | Uniform Manifold Approximation and Projection |
| VSELs | very small embryonic like stem cells |

## Introduction

Endothelial progenitor cells (EPCs) are described as a subpopulation of circulating $CD34^+$ and/or $CD133^+$ stem cells (SC) expressing mainly VEGFR-2 receptor (KDR in human). Conventional flow cytometric immunophenotyping has been widely described and used in most cases 3 to 4 markers (CD34, CD133, KDR, CD45) [1]. While EPCs origin remain controversial, we recently described that human bone marrow very small embryonic-like stem cells (VSELs) were able to differentiate into endothelial cells and to promote post-ischemic revascularization [2]. VSELs are major pluripotent SC defined as cells of small size being Lineage-negative, CD133-positive or CD34 positive, and CD45-negative [3]. Since EPCs and VSELs are extremely rare and their exact phenotype is still a matter of debate, more information with multiparametric proteomic is essential to decipher their exhaustive pattern. Mass cytometry (CyTOF) offers an interesting approach to address this issue, as it allows the simultaneous analysis of millions of cells with up to 40 metal tagged antibodies [4]. Since EPCs and/or VSELs can be mobilized in several ischemic or regenerative situations [2, 5], we addressed their characterization using a multidimensional proteomic single-cell approach in two different clinical settings.

First, stem and/or progenitor cells mobilization could be observed after implantation of bioprosthetic materials to acquire hemocompatibility. Indeed, Carmat bioprosthetic total artificial heart (C-TAH) is a biventricular pump that has been developed for end-stage heart failure patients [6]. We previously demonstrated an acquired hemocompatibility with a progressive endothelialization of the device membrane [7]. We hypothesized that endothelial cells found in the C-TAH come from the circulating blood since there is no physical connection between the device and patient blood vessels. Second, stem and/or progenitor cells mobilization can be observed during infection. Coronavirus 2 of Severe Acute Respiratory Syndrome (SARS-CoV-2) infection leading to the coronavirus disease 2019 (COVID-19) is a respiratory infection with a significant impact on the hematopoietic system [8]. We and others have shown that SARS-CoV-2 virus infect blood vessels and induce vascular damage [9–12]. The level of stem and/or progenitor cell mobilization in this context of viral infection associated to cytokine storm and endothelial lesion is currently unknown.

The aim of the study was to identify the distribution and phenotype of immune and potential circulating vasculogenic SC after C-TAH implantation known to be endothelialized by circulating cells [7]. We demonstrated existence of those mobilized candidates in COVID-19 patients (moderate versus critical ill patients) by reference to the most immature compartment- i.e. cord blood. This approach is based on robust protocols of cytometry (mass, imaging and flow) and provide exhaustive phenotype of vasculogenic stem and progenitor cells for human clinical studies and models of vascular disease.

## Methods

### Carmat Bioprosthetic Total Artificial Heart (C-TAH) Study Design and Population

The patient presented here was included in a single-arm, prospective, non-blinded, non-randomized study conducted in 4 French centers as previously described [6]. The study was registered in the European Databank on Medical Devices (CIV-FR-13-09-011615). Here we report stem/progenitor cell mobilization in a 58-year-old man with dilated cardiomyopathy. Peripheral blood samples were collected on EDTA before (T1 at day 0), one week (T2 at day 6) and two weeks (T3 at day 13) after C-TAH implantation. Ficoll isolated peripheral blood mononuclear cells (PBMNCs) were isolated, aliquoted, frozen and stored to assess deep immune phenotype by mass cytometry.

### COVID-19 Study Design and Population

Consecutive patients referred to emergency department of Georges Pompidou European hospital in Paris (France) with suspected SARS-CoV-2 infection were prospectively included. Here we analyzed stem and progenitor cell signatures 7 days after first symptoms for all patients ($n = 5$ per group). Clinical and biological characteristics of patients included are described in Supplementary Tables 1 and 2. SARCODO study was performed in accordance with the Declaration of Helsinki. All patients provided written informed consent before enrollment (CPP 2020–04-048 / 2020-A01048–31 / 20.04.21.49318).

### Mass Cytometry

Defrost peripheral blood mononuclear cells (PBMNCs) or cord blood mononuclear cells (CBMNCs) from density gradient centrifugation were re-suspended at a concentration of $10^7$ cells/ml and stained with Cisplatin 5 μM for 5 min (min) at room temperature (RT) to assess viability. After incubation with Fc Block, surface staining was performed by adding a cocktail of pre-conjugated and homemade-conjugated antibodies (Supplemental Table 3) for 30 min at RT as previously

described [13] and detailed in supplementary methods. Mass cytometry data were normalized using MatLab methods. For data cleaning, live cell population was extracted as a new .fcs file and uploaded on Cytobank platform to run unsupervised analysis using Spanning-tree Progression Analysis of Density-normalized Events (SPADE) algorithm. SPADE algorithm [14] generates trees illustrating the hierarchical relationship between clusters of cells based on a density-dependent down-sampling followed by agglomerative clustering to prevent rare cells from being overlooked among the more abundant cellular population. Based on the same clustering approach, $CD34^+$ population was analyzed with the Hierarchical Stochastic Neighbor Embedding (HSNE) algorithm designed to identify rare cell populations and to visualize cellular distribution with a density-based mode. HSNE dimension reduction-based algorithm generates a hierarchical representation that keeps the non-linear high-dimensional relationships between cells based on the similarity of all marker expressions simultaneously. As not mandatory, we choose not to perform down sampling step. The HSNE is implemented in the integrated single-cell analysis framework Cytosplore+ HSNE.

### Imaging Cytometry

CBMNCs samples were thawed slowly and resuspended in FACS Buffer for counting. Fluorescent staining (complete, monocolors and fluorescent minus one controls FMOs) were performed at 4 °C with Fc Block and for 30 min with anti-human antibodies cocktail of anti-lineage, CD45, CD14, CD19, CD34, CD133, VEGFR2 and Zombie dye (Supplemental Table 4). Cells were washed prior to acquisition with ImageStreamX at 60x magnification, low speed and high sensitivity.

Imaging flow cytometry data were analysed with IDEAS software. Cells were first selected by being well focused (Gradient-RMS of Brightfield channel), then singlets were selected using Brightfield Area and Aspect Ratio. Dead cells were excluded by Zombie NIR positive staining. $CD34^+$ and $KDR^+$ cells were identified based on respective patterns for CD14 and CD19 according to FMOs controls.

### Flow Cytometry

PBMNCs and CBMNCs samples were thawed slowly and resuspended in FACS Buffer for counting. Fluorescent staining was performed at 4 °C with Fc Block and for 30 min with anti-human antibodies cocktail of anti-lineage, CD45, c-Kit, CD19, CD34, CD133, VEGFR2 and Zombie dye (Supplemental Table 4). Cells were washed and fixed prior to acquisition with BD Fortessa Cytometer.

Data were first analyzed in a supervised way with FlowJo to perform live lineage negative cells down sampling and concatenation of the subsequent files. Uniform Manifold Approximation and Projection (UMAP) algorithm [15] was performed to apply dimension reduction to the data while well preserving their global structure.

### Statistical Analysis

Continuous data were expressed as median [interquartile range: (IQR)] and categorical data as proportion. Patients were compared according to level of care (hospitalization in conventional medical unit or hospitalization directly in ICU). In univariate analysis, we determined the differences in median using the unpaired t-test (Mann-Whitney U test) for continuous variable and differences in proportions were assessed with the Chi-square test or Fischer exact test if necessary. All analyses were 2-sided and a $p$ value of $p < 0.05$ was considered statistically significant. Statistical analysis was performed using R studio software (R Development Core Team (2019). R: A language and environment for statistical computing. R Foundation for Statistical Computing, Vienna, Austria).

## Results

### Bioprosthetic C-TAH Implantation Induces Redistribution of Circulating Immune Cells and Mobilization of SC in Peripheral Blood

PBMNCs from C-TAH implanted patient were successively collected before (T1) and after surgery (T2 and T3). Deep immunophenotyping by mass cytometry was performed to assess circulating immune populations and to focus on stem and progenitor cell subsets which play a key role in neo-vascularization. Using mass cytometry data, unsupervised SPADE algorithm was applied to design trees in order to identify major circulating populations. Figure 1a illustrates the distribution of the immune circulating populations identified based on sequential expression patterns for multiple clusters of differentiation. In Fig. 1b, a drastic reduction in circulating $CD4^+$ T-lymphocytes was observed one week post-engraftment with a return to basal values at two weeks while the level of $CD8^+$ T-lymphocytes remained equal over time. $CD19^+$ B-lymphocytes population showed a strong increase one week after implantation before going back to pre-implantation level at T2. Natural killer (NK) $CD56^+$ cells were divided into two subpopulations according to $CD57^+$ expression related to their activation status. Both activated and non-activated NK cell populations displayed the same percentages and patterns of evolution over time points with a slight increase at T3. Classical $CD14^+CD16^-$ monocytes were mobilized one week after C-TAH implantation while pro-

inflammatory intermediate and non-classical monocytes $CD16^+$ remained at very low levels. After 2 weeks at T3, classical monocytes tended to pre-implantation levels while $CD14^-CD16^-$ tended to slightly increase. Figure 1c, the sub-population of circulating $CD34^+$ increased by 1.35 fold two weeks after transplantation. Thus, $CD34^+$, $CD19^+$ and $CD14^+$ sub-populations were mobilized in peripheral blood after C-TAH implantation.

## Circulating $CD34^+$ Cells Are Negative for KDR

The three mobilized subpopulations $CD34^+$, $CD19^+$ and $CD14^+$ populations were extracted from the circulating cells SPADE trees from C-TAH patient and concatenated per time-point to design a stem cell and progenitor focused SPADE tree (Fig. 2a). Eight subpopulations were subsequently identified based on their differential phenotype considering the positivity for CD34, CD133, CD45, CD14, CD11c, CD19 and CD20 markers. Among the $CD34^+$ populations, four sub-populations were identified based on their respective expression of CD133 and CD45 – i.e. $CD34^+CD45^-CD133^-$, $CD34^+CD45^-CD133^+$, $CD34^+CD45^{dim}CD133^-$ and $CD34^+CD45^{dim}CD133^+$. Then, CD14 expressing monocytes were divided in two sub-populations according to CD11c levels – i.e. $CD14^+CD11c^+$ and $CD14^+CD11c^{low}$ - while B-lymphocytes were sorted on presence or absence of CD20 expression – i.e. $CD19^+CD20^-$ and $CD19^+CD20^+$. For each sub-population, expression level of markers of stem cells (Oct-3/4, c-Kit, FcεR1, CD13 and CD49F), mesenchymal cells (CD90) and endothelial cells (KDR) were assessed at T1 as well as those of CD31 (PECAM-1) expressed by endothelial and leukocyte subsets and CD105 (endoglin) expressed by mesenchymal lineage.

The same strategy was applied to selected $CD34^+$, $CD19^+$ and $CD14^+$ subpopulations from healthy PBMNCs and CBMNCs samples and identified by mass cytometry.

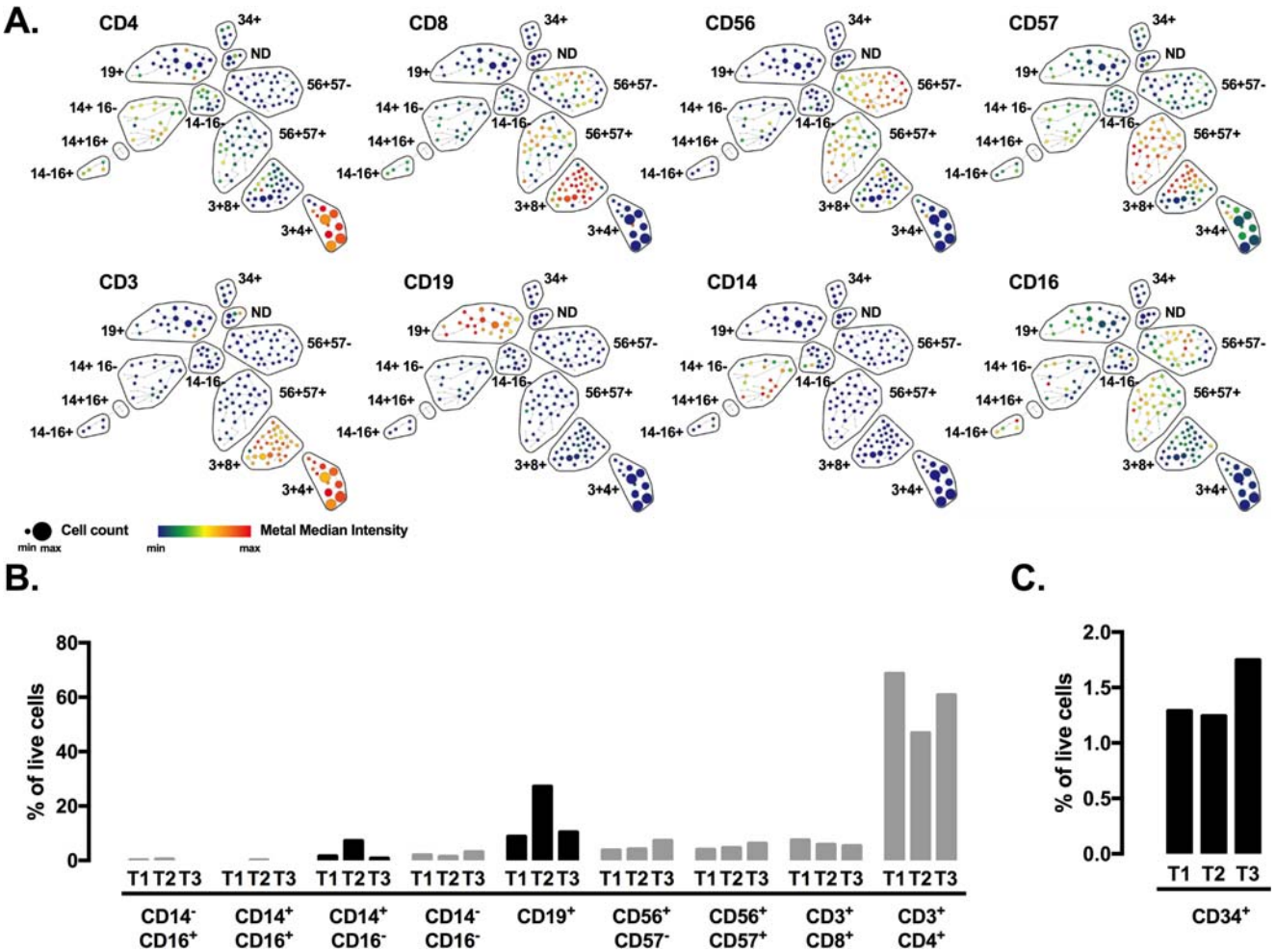


**Fig. 1** Redistribution of circulating immune cells in peripheral blood after C-TAH implantation. a Identification of live peripheral blood nuclear cell populations using SPADE unsupervised analysis and displayed by major immune markers. b Evolution overtime of major lymphoid and myeloid cell populations, expressed in percentages of live cells. c Level of $CD34^+$ cells expressed in percentages of live cells overtime

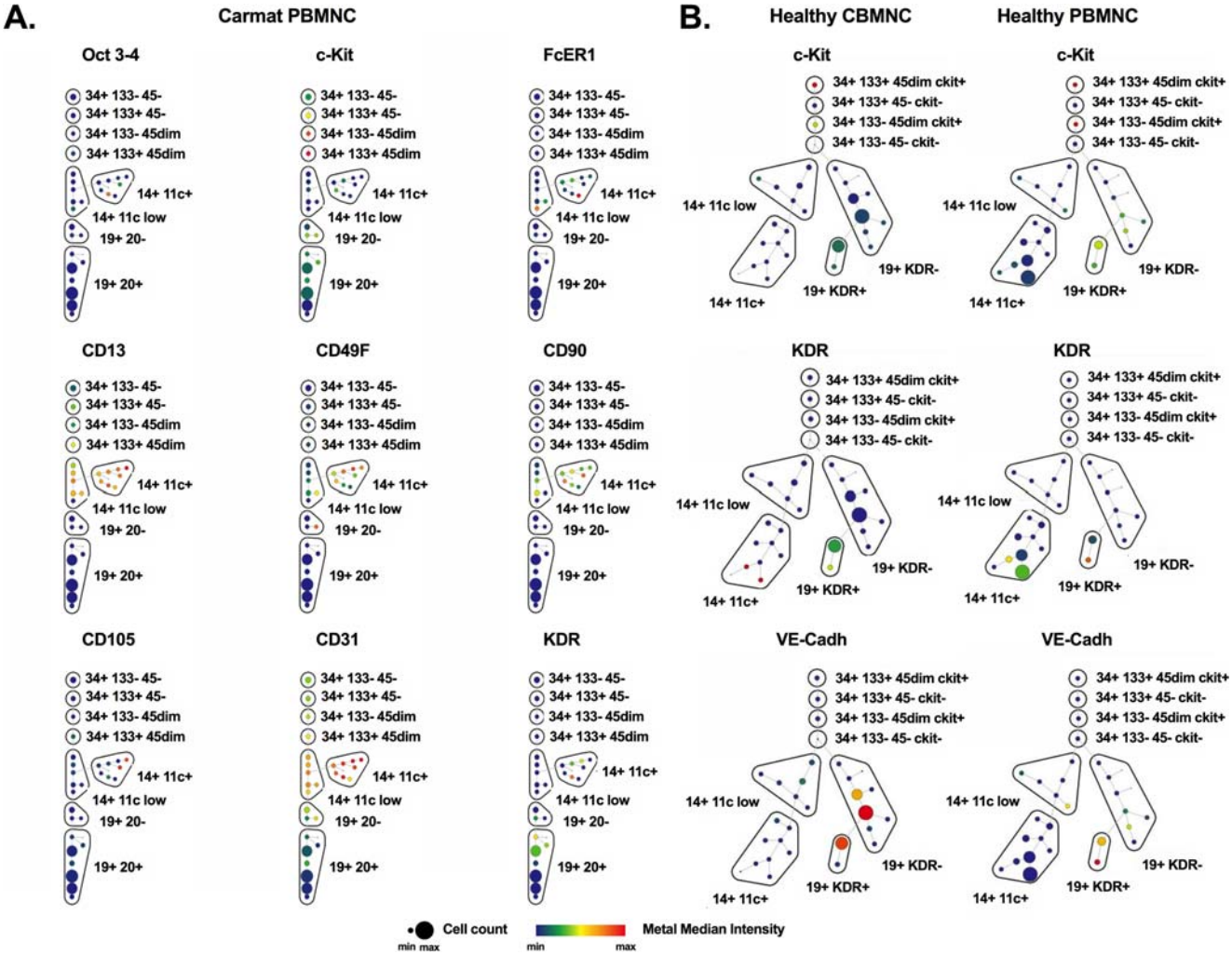


**Fig. 2** Expression of stem, mesenchymal and endothelial markers in CD34+, CD19+ and CD14+ sub-populations. a Phenotypical signature within stem cell and progenitor focused SPADE tree in CD34+, CD19+ and CD14+ sub-populations of C-TAH patient at T1. b Phenotypical signature within stem cell and progenitor focused SPADE tree in CD34+, CD19+ and CD14+ sub-populations of healthy CBMNCs and PBMNCs

Cellular profiles observed with C-TAH were confirmed in healthy samples in Fig. 2b and expression of c-Kit, KDR and VE-Cadherin assessed endothelial pattern of CD19+ cells by revealing VE-Cadherin expression in $CD19^+$ cells and its absence in $CD34^+$ cells.

In C-TAH patient, kinetic of expression for selected markers was then assessed per subpopulation as.illustrated at T1 (basal expression levels) in Fig. 3 with black bars scaled on the maximal expression per marker among populations from the stem/progenitor cells focused SPADE tree. At T1, all $CD34^+$ sub-populations expressed c-Kit, CD13 and CD49F SC markers as well as CD31 but only the $CD133^+$ expressed Oct-3/4 stem transcription factor. None of the $CD34^+$ stems and progenitor populations expressed the KDR by contrast to $CD19^+$ and $CD14^+CD11c^{low}$ sub-populations that showed also positive expressions for some stem, mesenchymal or endothelial markers. Thus, prior to implantation of C-TAH, KDR was only expressed by $CD19^+$ B-lymphocytes and $CD14^+$ monocytes subpopulations but not by $CD34^+$ subpopulations in circulation.

$CD34^+c\text{-}Kit^+$ progenitor cells are mobilized after C-TAH implantation.

Expression variations for discriminative marker to T1 over T2 and T3 time-points are illustrated for each sub-population in the Fig. 3 heat-map with a color code (blue decrease / white stability / red increase). Over the kinetic, positive expressions of KDR remained identical in $CD19^+$ cells and increased in both $CD14^+$ sub-populations while keeping a negative expression in all the $CD34^+$ sub-populations. Independently of CD133 and CD45 levels of expression, $CD34^+$ sub-populations showed the same variation pattern of expression along time points with an increase of CD13 and CD31 at T2 before a decrease at T3. While the $CD34^+CD45^-CD133^-$ never expressed

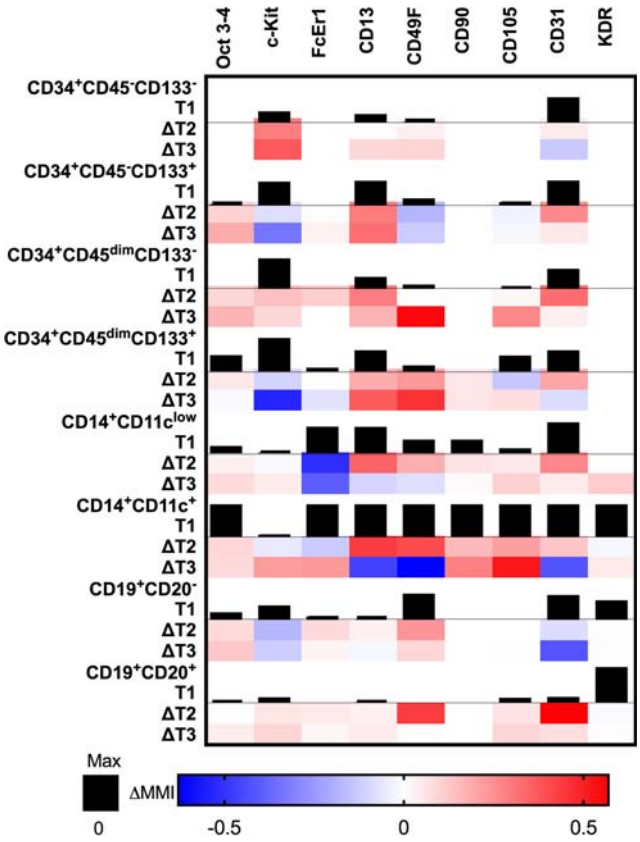


**Fig. 3** Evolution of stem, mesenchymal and endothelial markers over time in mobilized $CD34^+$, $CD19^+$ and $CD14^+$ sub-populations. Pre-implantation (T1) levels of maximal relative expression for clusters of differentiation and transcription factors sorted by population subsets (black bars) associated to post-implantation variation (heat-map with a color code: blue decrease / white stability / red increase) expressed in Median Metal Intensity relative variation to T1 (ΔT2, ΔT3)

Oct3/4 and CD105, other sub-populations displayed an increase of both markers over time. CD105 mesenchymal marker is increasing within the $CD45^{dim}$ sub-populations whereas c-Kit stem marker is increasing only within the $CD133^-$ stem/progenitor sub-populations whatever $CD45^-$ or $CD45^{dim}$ expression.

We further explored the display of CD34, CD133 and CD45 with the HSNE map in Fig. 4a of merged T1, T2 and T3, $CD34^+$ populations allows, based on differential patterns of intensities, the identification of four $CD34^+$ subsets with expression profiles A, B, C and D confirming those previously identified (respectively A: $CD34^+CD45^-CD133^-$, B: $CD34^+CD45^-CD133^+$, C: $CD34^+CD45^{dim}CD133^-$ and D: $CD34^+CD45^{dim}CD133^+$). To identify all of the populations represented through the different kinetic times, it is necessary to consider the data as a whole by pooling all the points making it possible to highlight each of the populations independently of their presence / absence at a given time. This approach that does not rely on kinetic attests the global absence of expression of KDR in $CD34^+$ cells and confirms the ability of the $CD34^+CD45^{dim}$ cells to highly express c-Kit. Among $CD34^+$ population, the HSNE cellular density visualization per time point in Fig. 4b underlines the redistribution of the four $CD34^+$ subsets as quantified in Fig. 4c and emphasizes a mobilization of the $CD34^+CD45^{dim}$c-$Kit^+$ whatever expression of CD133. None of stem/progenitor populations mobilized after C-TAH implantation expressed KDR.

## $CD34^+$c-$Kit^+$ Progenitor Cells Are Mobilized in COVID-19 Critical Patients

Since COVID-19 has been described as hypoxic condition associated with strong vascular dysfunction, we decided to explore cells phenotype characterized in mass cytometry previously in a 10 COVID-19 patients cohort with moderate and critical severity.

Supervised analysis of flow cytometry data confirmed the presence of the previously identified $CD34^+$ subpopulations based on their CD45, CD133 and c-Kit expression in peripheral blood of both groups of COVID-19 patients as well as in healthy cord blood samples. The statistical analysis showed, in a first approach, that among the four populations of $CD34^+CD45^{-/dim}CD133^{-/+}$, only the $CD34^+CD45^{dim}CD133^+$ was significantly mobilized ($p = 0.022$) in COVID-19 critical patients compared to moderate ones (Fig. 5a-d). The $CD34^+CD45^{-/dim}CD133^{-/+}$ populations could be sub-divided into two categories according to the positivity of c-Kit. There was no difference between moderate and critical COVID-19 in the $CD34^+CD45^-CD133^{-/+}$c-$Kit^{-/+}$ (Fig. 5b-c). A highly significant increase of the $CD34^+CD45^{dim}CD133^+$c-$Kit^+$ ($p = 0.008$) was observed (Fig. 5f) while no difference existed in the $CD34^+CD45^{dim}CD133^+$c-$Kit^-$ population (Fig. 5e). To identify stem and progenitor cells expressing KDR in COVID-19 and CB-MNCs samples among the selected live lineage negative cells, four populations based on distinct patterns of both CD34 and KDR were assessed as illustrated in Fig. 5g and respective profile for CD45 and CD133 were observed. We observed that, regardless CD34 level, KDR+ cells are 100% $CD45^{high}$ expressing cells.

## $CD34^+$ $KDR^+$ $CD19^-$ Are all Non-circular Events

Consensual phenotypic definition of circulating EPCs relies on expression of CD34 and KDR markers simultaneously. First, we have shown in COVID-19 patient peripheral blood that KDR was only expressed by $CD45^{high}$ cells, and second, that in peripheral blood of C-TAH patient, KDR was only expressed by B cells and monocytes, both $CD45^{high}$ expressing cells. Therefore, we analyzed the phenotype of from cord-blood for CD14 and CD19 markers by imaging flow cytometry that enable us to localize fluorescence and to have a clear picture of the cells morphology on the top of conventional flow cytometry data. As illustrated in the gating strategy of the Fig. 6a, $CD34^+KDR^+$ focused live circular single cells are

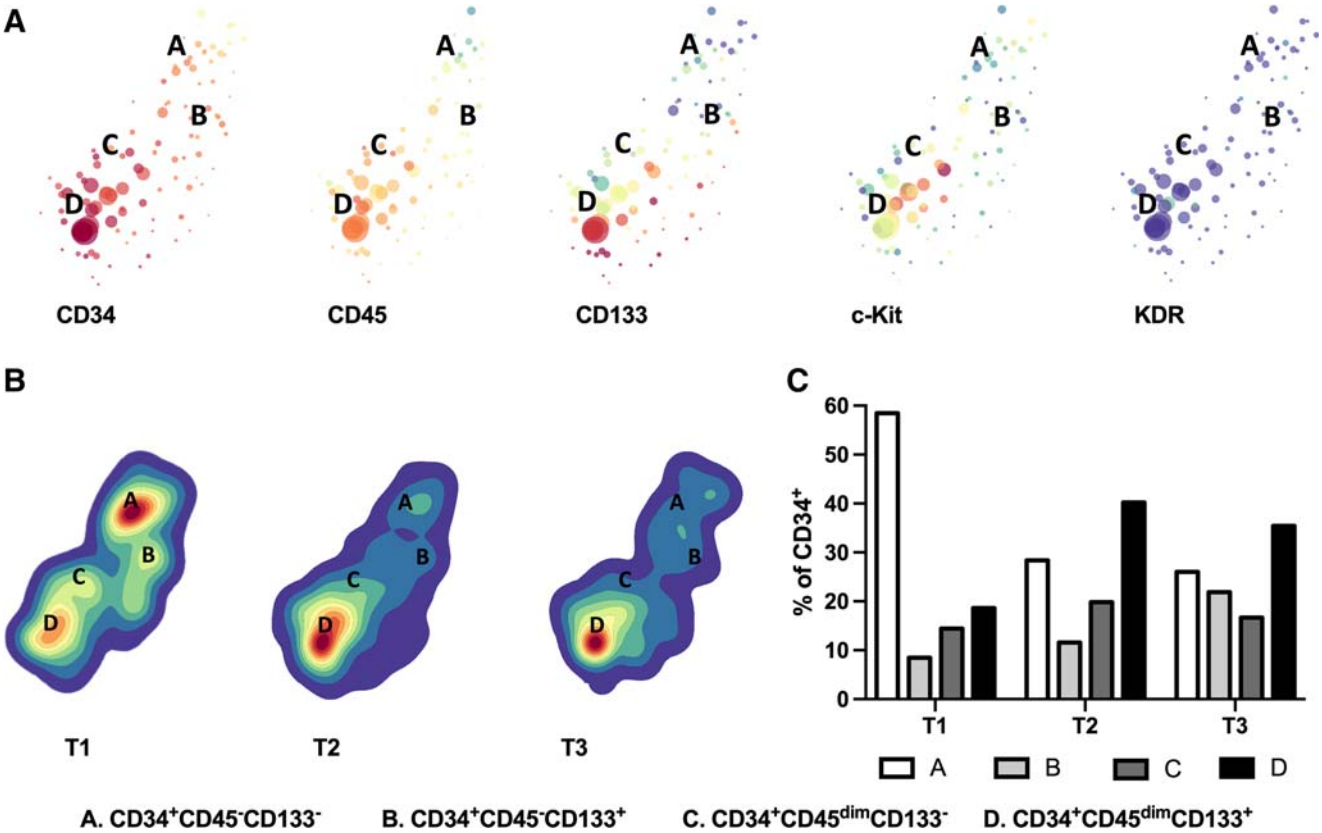


**Fig. 4** Mobilization of stem cells in peripheral blood post C-TAH implantation. a Cartography of $CD34^+$ sub-populations identified as **a**, **b**, **c** and D based on their CD133 and CD45 differential patterns and correlated with KDR and c-Kit expression using unsupervised HSNE algorithm. A: $34^+45^-133^-$, B: $34^+45^-133^+$, C: $34^+45^{dim}133^-$ and D: $34^+45^{dim}133^+$. b Distribution profiles of HSNE mapped $CD34^+$ subsets visualized in cell density at T1, T2 and T3. c C Repartition of A, B, C and D populations over time points

positive only for CD19 marker. Some non-circular events were expressing the double positivity for CD34 and KDR but, based on their shape in Fig. 6b, were not intact biological events of interest as cells in suspension from cord blood are expected to be round. Figure 6c and d confirm that in circular events, all cells positive for KDR were $CD19^+$ cells whatever expression of $CD34^+$.

### $CD19^+KDR^+$ Cells Are Mobilized in COVID-19 Critical Patients

Flow cytometry analysis performed on moderate and critical COVID-19 MNCs from peripheral and healthy cord blood samples showed a comparable level of $CD19^+$ whatever the expression of CD34 in each group (Fig. 7a). A significant mobilization of $CD19^+KDR^+$ per million of $CD45^+$ cells was observed between moderate and critical COVID-19 patients ($p < 0.001$) in Fig. 7b, regardless of CD34 level, negative ($p < 0.0001$) or positive ($p = 0.001$). Data of the resulting clusters are visualized on a UMAP plot in Fig. 7c showing all single cells of the live lineage negative events selected from down sampled files concatinated per group where $CD19^+$ $KDR^+$ population from respective group are overlapped in blue on the UMAP.

## Discussion

Using a multidimensional proteomic single-cell approach, we analyzed two different clinical models of cardiovascular disease with $CD34^+$ mobilization and demonstrated (i) that a subset of these cells was $CD34^+$c-$Kit^+KDR^-$, and (ii) that all cells positive for VEGFR-2/KDR cells in peripheral blood were CD19-positive questioning the potential involvement of CD19/B-lymphocytes in cardiovascular and infectious diseases.

This study was motivated by data from the past 20 years aiming at identifying EPCs in blood by conventional flow cytometry approaches. Authors generally defined EPCs as cells positive for the KDR in the lymphocyte gate. However, this cell population can be challenged since no correlation has been reported between the number of these circulating cells and the number of endothelial colonies forming cells (ECFCs) obtained in cell culture [16, 17]. Of note, ECFCs are considered by

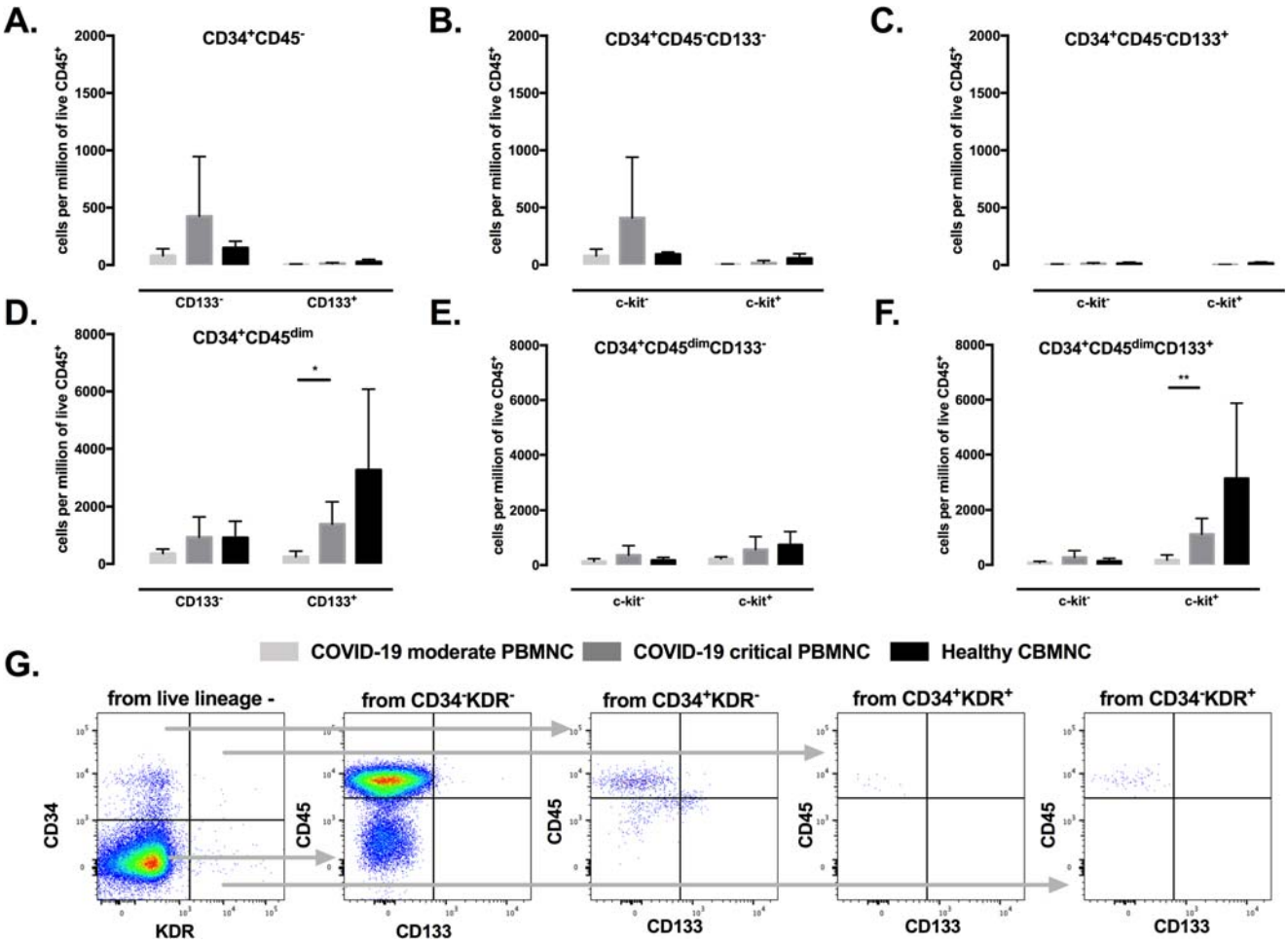


**Fig. 5** Mobilization of stem cells in peripheral blood in critical COVID-19 patients. **a** Quantification of $CD34^+CD45^-CD133^+$ or $CD133^-$ cells expressed per million of live $CD45^+$ cells in peripheral blood of COVID-19 moderate and critical patients and in healthy cord blood samples. **b** Quantification of c-$Kit^+$ or c-$Kit^-$ cells among the $CD34^+CD45^-CD133^-$ population. **c** Quantification of c-$Kit^+$ or c-$Kit^-$ cells among the $CD34^+CD45^-CD133^+$ population. **d** Quantification of $CD34^+CD45^{dim}CD133^+$ or $CD133^-$ cells expressed per million of live $CD45^+$ cells. **e** Quantification of c-$Kit^+$ or c-$Kit^-$ cells among the $CD34^+CD45^{dim}CD133^-$ population. **f** Quantification of c-$Kit^+$ or c-$Kit^-$ cells among the $CD34^+CD45^{dim}CD133^+$ population. **g** Illustration of CD45 and CD133 expressions according distinct patterns for CD34 and KDR of live lineage negative cells in peripheral blood of COVID-19 patients - Among the live cells, each of the 4 populations based on respective expressions of CD34 and KDR are phenotype on the CD45 and CD133 markers thus illustrating that all the $KDR^+$ events are exclusively $CD45^{high}$ $CD133^-$ $^*p < 0.05$; $^{**}p < 0.01$.

consensus as true endothelial progeny derived from circulating progenitors [18]. In a recent meta-analysis reporting pooled data on the association between levels of circulating progenitor cells, cardiovascular outcomes and death, $CD34^+$ and $CD34^+CD133^+$ were the most frequent cell population associated with cardiovascular outcomes and death. $CD34^+$ were therefore proposed as the best candidate for a clinical-grade biomarker of cardiovascular risk [19]. However, the pathophysiology link between $CD34^+$ vasculogenic potential and outcomes remain largely speculative.

Interestingly, we described a progressive endothelialization of the bioprosthetic membrane of the C-TAH that could be at the origin of its acquired hemocompatibility [7]. Since there is no physical connection to between membrane bioprosthesis to patient blood vessels, the source of these neo-endocardial cells in the C-TAH would come from the circulating blood. In the present study, one patient receiving C-TAH could be explored at different time-points; we evidenced a mobilization of $CD34^+$ cells by mass cytometry analyzed with SPADE algorithm. It provided a unique opportunity to comprehensively characterize circulating vasculogenic stem and progenitor cells at the single cell level in a complex environment. After implantation of bioprosthetic total artificial heart, we show a global increase of CD133 stem marker in all $CD34^+$ cells associated to an increase over time of Oct3/4 and c-Kit in $CD34^+CD133^+$ cells subpopulations. Thus, newly formed endothelial cells observed on top of bioprosthetic tissue inside C-TAH could be issued from this $CD34^+$c-$Kit^+$ subpopulation. Indeed, $CD34^+$c-$Kit^+$ populations have already been

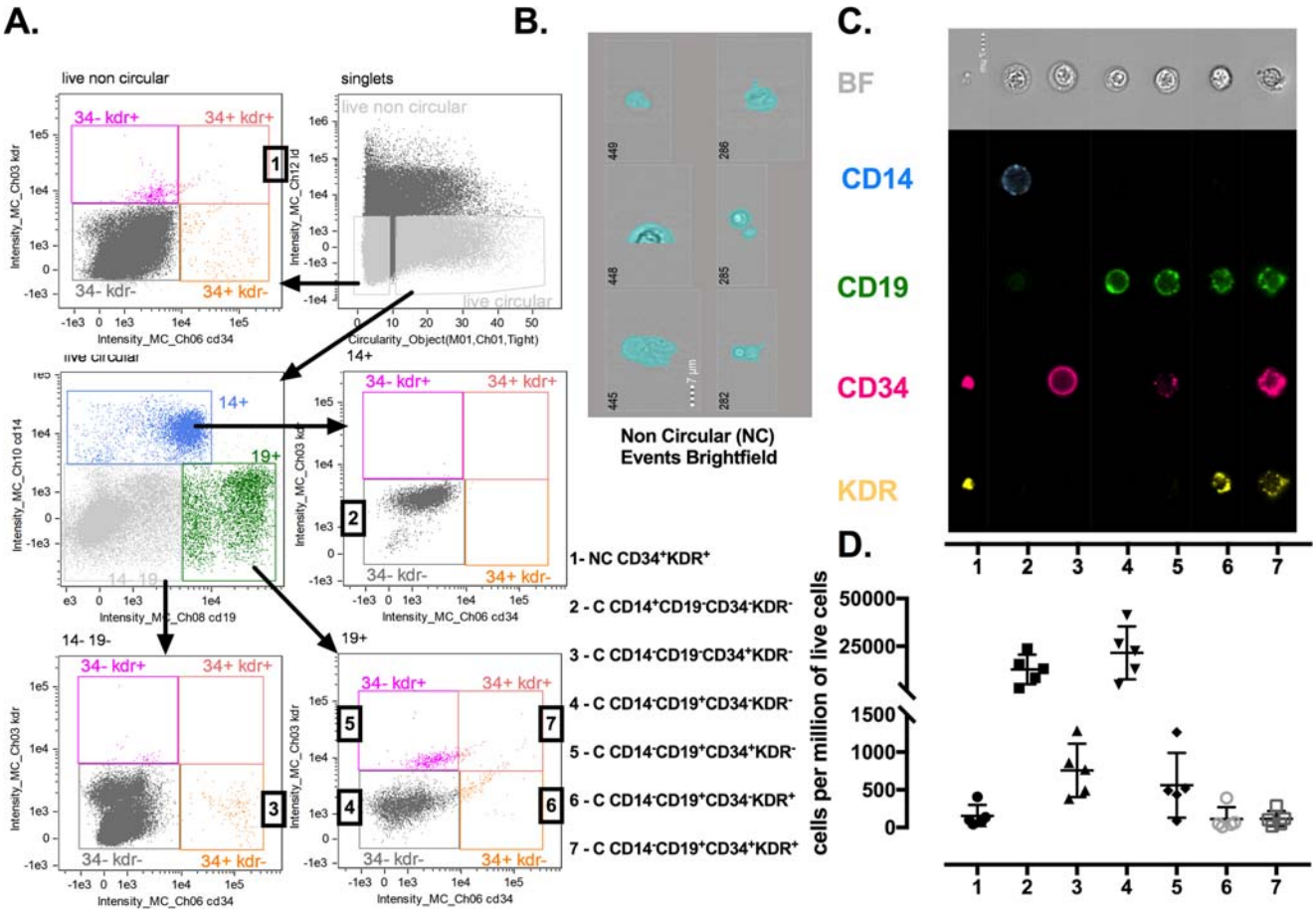


**Fig. 6** $CD34^+KDR^+$ phenotypic analysis in cord blood by imaging cytometry. a Image flow cytometry gating strategy (focus/singlets/live circular/ CD14 or CD19 / CD34 or KDR) with identification of several populations as non-circular (NC) in 1, circular (C) $CD14^+$ in 2, C $CD14^-CD19^-CD34^-KDR^-$ in 3 and $CD34^+KDR^-$ in 4, C $CD14^-CD19^+CD34^-KDR^-$ in 5 and $CD34^-KDR^+$ in 6 and the last C $CD14^-CD19^+CD34^+KDR^+$ in 7. b Visualization of the brightfield of the non-circular events by imaging flow cytometry. c Visualization of the non-circular and circular events from population 1 to 7 by imaging flow cytometry and associated phenotype for CD14, CD19, CD34 and KDR. d Quantification of populations 1 to 7 per millions of live cells in CBMNCs

described to have endothelial differentiation potential in vivo [20] and $CD133^+$c-$Kit^+lin^-$ cells from human cord blood have also already been described to have ability to differentiate in ECFCs [21]. Potential mobilization of these cells in critical COVID-19 could provide endothelial regeneration helpful during hypoxia observed in COVID-19 patients [22, 23], but on the other hand could participate to dissemination of thrombotic profile observed in clinic [8]. Indeed, we recently described that ECFCs can be potential actor of procoagulant process [24].

Surprisingly, with our multiparametric analysis, we were not able to identify circulating EPCs usually defined as $CD34^+KDR^+$ in peripheral blood. Herein, mass and imaging flow cytometry panels demonstrated that all KDR positive cells are either B-lymphocytes $CD19^+$ or monocytes $CD14^+$ in patient's peripheral blood and healthy peripheral and cord blood. KDR expression in monocyte could correspond to so-called early-EPC (circulating angiogenic cells) well described in early 2000 in particular by Dimmeler's group. This subpopulation is able to modify angiogenic process by secreting growth factors but has not the ability to form endothelial cells in culture [5].

KDR has been described in hematopoietic stem cells (HSCs) to play a crucial role in hematopoiesis [25]. HSCs have been described to be in $CD34^+KDR^+$ cell fraction defining KDR as a positive functional marker for HSCs, without definition of their CD19 status. Our results demonstrate that KDR is expressed by $CD19^+$ cells (that are supposed to be B lymphocytes) and monocytes, without any significant modulation after C-TAH implantation in contrast to critical form of COVID-19. We confirmed our results in CB-MNCs with a flow cytometry approach and studying circularity of single cells. As described here, $CD34^+KDR^+$ are mostly debris [26] and/or non-circular events whose size is compatible with flow gating strategy including lymphocytes used in most of previously performed clinical studies. Thus, we confirmed

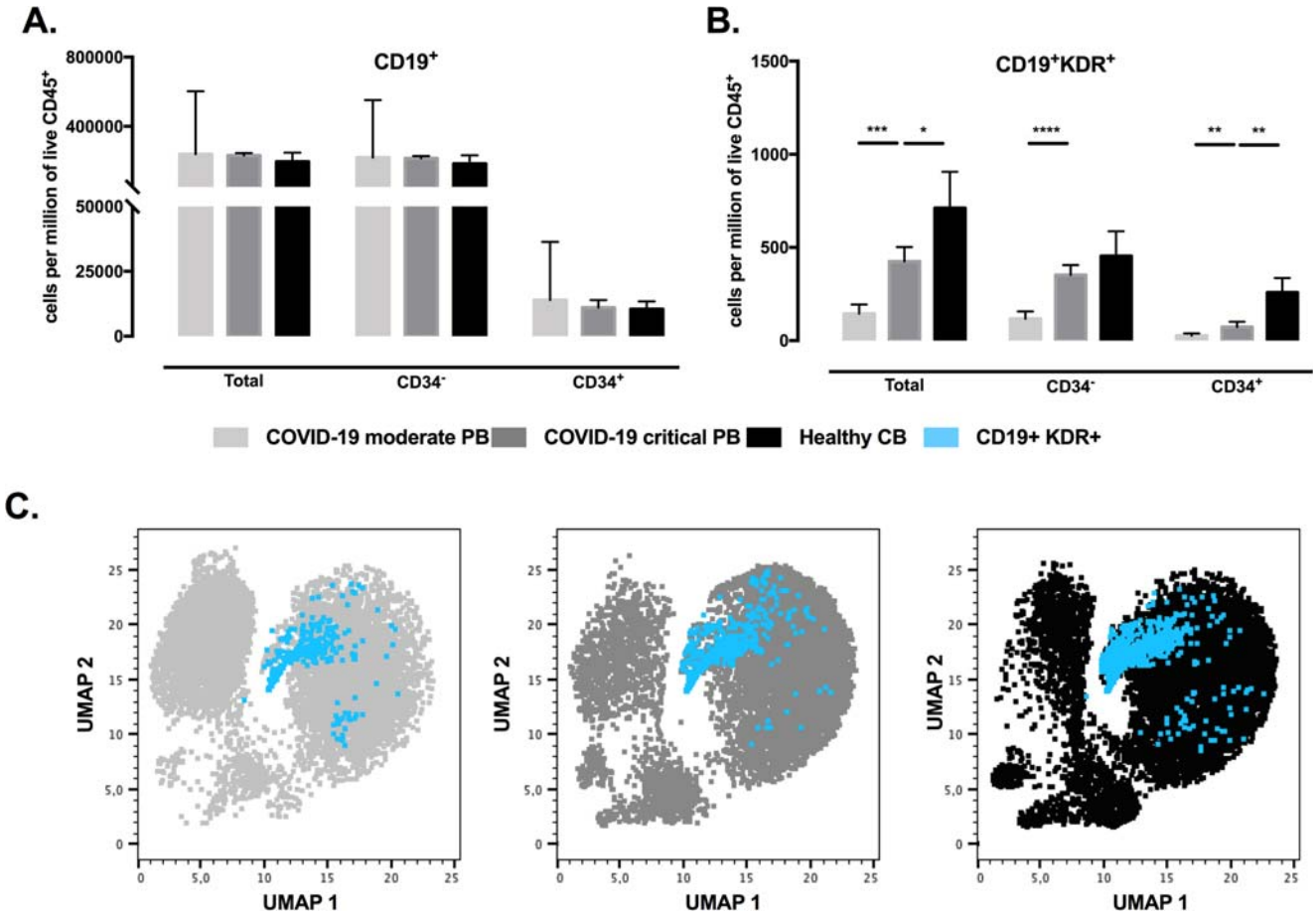


**Fig. 7** $CD19^+KDR^+$ cells are mobilized in peripheral blood of COVID-19 critical patients. a Quantification of $CD34^-$ and $CD34^+$ cells of the $CD19^+$ population and expressed per million of live $CD45^+$ cells in peripheral blood of COVID-19 moderate and critical patients and in healthy cord blood samples.b Quantification of $CD34^-$ and $CD34^+$ cells of the $CD19^+KDR^+$ population and expressed per million of live $CD45^+$ cells. c UMAP visualization of the $CD19^+KDR^+$ (in blue) of down sampled live lineage negative population concatenated per condition, ie COVID-19 moderate (light grey) COVID-19 critical (dark grey) and healthy cord blood (black).*p < 0.05; **p < 0.01; ***$p < 0.001$; ****$p < 0.0001$

that KDR is never expressed on circular CD19 negative cells, whatever expression of $CD34^+$ cells. In cord blood, circular $CD34^+KDR^+$ are all $CD19^+$. $CD34^+CD19^+$ are rare event in peripheral blood supposed to be pre-B cells [27]. Thus, in conventional flow, cell circularity is not assessed. This circularity feature is crucial parameter for identification of circulating rare events. $CD19^+$ cells are involved in both innate and adaptive immune responses through both antibody-dependent and antibody-independent mechanisms. B lymphocytes have been proposed leading to enhanced myocardial inflammation, tissue injury and deterioration of myocardial function [28]. Our new data proposing that KDR cells are CD19 cells reshuffle the cards of EPCs involvement in cardiovascular field and also emphasize involvement of B cell in cardiovascular events and death [29].

We confirmed all phenotype of $CD34^+$ and $CD19^+$ cells observed in C-TAH patients in healthy peripheral and cord blood with mass cytometry and demonstrated their existence in COVID-19 patients. COVID-19 is a respiratory infection with a significant impact on the hematopoietic system and hemostasis [8]. Current hallmarks of COVID-19 are the cytokine storm, coagulopathy and endothelial dysfunction [8]. This cytokine release syndrome in COVID-19 patients is associated to a decreased count of lymphocyte [30]. This lymphopenia has been related to a significant decrease in T cells (in particular $CD8^+$ T cells) and this significant decrease of T lymphocyte subset is positively correlated with in-hospital death and severity of illness [8]. Here we show that total $CD19^+$ cells are not modulated in COVID-19 patients along the disease, while $CD19^+KDR^+$ cells are increased in critical form in contrast to moderate form of the disease. B lymphocytes have also been proposed to be involved

in COVID-19, since patients with a gammoglobulinemia lacking B lymphocytes had a mild clinical course in contrast to COVID-19 patients with common variable immune deficiency [31]. Thus, phenotyping approach enabled us to identify a new circulating actor positive for the CD19 antigen associated with an endothelial $KDR^+$ and VE-$cadh^+$ phenotype. Future work will assess the role of the $KDR^+$ and endothelial lineage marker along the B progeny, in particular in human B cell memory, as actor or as key mediator in lymphopoïesis and/or vasculogenic processes.

We found that mobilized $CD34^+CD133^+$ cells after C-TAH implantation are enriched in c-Kit expression. Human or mouse c-Kit SC from different organs have been described to be able to differentiate into endothelial cells [32]. Before C-TAH implantation, c-Kit is expressed in all $CD34^+$ cells. After implantation, c-Kit decreases in the $CD133^+$ cells while it increases in $CD34^+CD133^-CD45^{-/dim}$ subpopulations. VSELs are major pluripotent small size SC defined in humans as Lineage-negative, CD133 positive or CD34 positive, and CD45 negative cells [3] but their exhaustive simultaneous phenotype for CD34 and CD133 is not yet well assessed. VSELs $CD133^+$ or $CD34^+$ have been shown in several studies to have multilineage differentiation ability into cells from different germ layers [3]. We and others have previously shown their ability to differentiate in endothelial cells [2]. $CD34^+$VSELs express c-Kit since KIT ligand have been recently described to enhance their expansion [3]. Thus, these $CD34^+CD133^-CD45^-$c-$Kit^+$ cells could correspond to VSEL and recolonize pericardial to form endothelial cells observed [7]. We also found that mobilized $CD34^+CD133^+CD45^-$ cells after C-TAH implantations are significantly enriched in oct3/4 expression. The only circulating cells expressing markers of pluripotent SC Oct-4 are VSELs. Indeed, Oct-4 positive VSEL have been described to express CD34 or CD133, and are negative for lineage markers and the pan-hematopoietic marker CD45 [3]. Thus, mobilization of c-Kit and oct3/4 positive cells could be reflecting VSEL mobilization after C-TAH implantation, and give rise to endothelialization of C-TAH membrane.

We also found $CD34^+CD133^+CD45^{dim}$c-$Kit^+$ cells mobilization in COVID-19 patients. Since endothelial lesion have been described in COVID-19 [9–12], mobilization of this stem cell subpopulation from bone marrow and/or vessels and/or white adipose tissue could be triggered by this vascular dysfunction or cytokine storm. Beyond vascularization repair, mobilization of multipotent SC c-$Kit^+$ and/or VSELs could help organs recovery in C-TAH and COVID-19 patients. Indeed, mesenchymal stem cells have been proposed to modulate inflammation around endothelial cells during COVID-19 and also cure endothelial dysfunction to accelerate their recovery after COVID-19 induced vascular lesion and are currently tested in COVID-19 [8] (Stroma-Cov-2 project: *NCT04333368*). Since c-$Kit^+$ and/or VSELs have the ability to support vasculogenesis and give rise to hematopoietic cells to counteract lymphopenia and inflammation, this stem/progenitor cell mobilization in COVID-19 could be triggered by infection to counteract side effect of virus infection.

## Limitation of the Study

Very small amount of $KDR^+$ cells induce lots of technical problems with large variations and variability in different groups and require large number of events scored by flow cytometry which was as well a limitation in our C-TAH samples containing maximum 1 million cells dedicated to mass cytometry acquisition. MNCs from COVID-19 and CB-MNC flow cytometry quantification were normalized in cells per million of $CD45^+$ cells to be compared but ficoll isolation of MNCs led to the loss of the neutrophils within samples. Our newly described populations of $CD34^+$c-$Kit^+$ and $CD19^+KDR^+$ need to be confirmed in larger cohort to explore correlation with cardiovascular outcomes. On a clinical point of view, C-TAH and COVID-19 patients explored here had heparin/LMWH therapy: in preventive dose in COVID-19 patients and therapeutic dose in C-TAH patient. We recently described anticoagulation as a preserving factor for endothelial lesion induced by COVID-19 [12]. Indeed, in 66 COVID-19 patients we found that patients with oral anticoagulation had a significant decrease in CECs. Thus, we cannot exclude an effect of heparin and/or LMWH on circulating endothelial compartment or their stem/progenitor cells.

In conclusion, bioprosthetic total artificial heart implantation and COVID −19 patients allowed us to fully characterize stem and progenitor cells in blood that could be at the origin of the endothelial recovery. Large phenotyping allowed us to demonstrate that non KDR cells with immaturity markers can be mobilized and confirmed absence of KDR on circulating stem/progenitor cells. This result needs to be explored to understand exact $CD19^+$ $KDR^+$ cells involvement in cardiovascular disease and endothelial differentiation.

**Acknowledgements** We would like to acknowledge all nurses, technicians and physicians involved in the Cardiac Surgery for C-TAH and Vascular medicine, Internal medicine, Respiratory medicine, Intensive care, Clinical investigation center and Hematology departments of the George Pompidou European Hospital in COVID-19 cohort for their help in taking care of patients and including them in the study. We thank AP-HP for promotion of the SARCODO Project. We thank the unit of clinical research URC HEGP CIC-EC1418 (Natacha Nohile, Pauline Jouany and Dr. Juliette Djadi-Prat) and Helene Cart-Grandjean from AP-HP for their involvement in SARCODO project.

**Funding** This work was supported by grants of the LIH, Carmat, PROMEX STIFTUNG FUR DIE FORSCHUNG foundation, ANR SARCODO, Fondation de France and Appel d'offre AP-HP mécénat crise COVID-19 From GHU APHP.CUP.

## Compliance with Ethical Standards

**Conflict of Interest** A Carpentier is cofounder and shareholder of CARMAT SA. DMS and CL received consulting fees from CARMAT. A Capel and P. Jansen are employed by CARMAT SA.

## References


1. Mund, J. A., Estes, M. L., Yoder, M. C., Ingram Jr., D. A., & Case, J. (2012). Flow cytometric identification and functional characterization of immature and mature circulating endothelial cells. *Arteriosclerosis, Thrombosis, and Vascular Biology, 32*(4), 1045–1053.
2. Guerin, C. L., Loyer, X., Vilar, J., Cras, A., Mirault, T., Gaussem, P., Silvestre, J. S., & Smadja, D. M. (2015). Bone-marrow-derived very small embryonic-like stem cells in patients with critical leg ischaemia: Evidence of vasculogenic potential. *Thrombosis and Haemostasis, 113*(5), 1084–1094.
3. Ratajczak, M. Z., Ratajczak, J., Suszynska, M., Miller, D. M., Kucia, M., & Shin, D. M. (2017). A novel view of the adult stem cell compartment from the perspective of a quiescent population of very small embryonic-like stem cells. *Circulation Research, 120*(1), 166–178.
4. Bendall, S. C., Nolan, G. P., Roederer, M., & Chattopadhyay, P. K. (2012). A deep profiler's guide to cytometry. *Trends in Immunology, 33*(7), 323–332.
5. Silvestre, J. S., Smadja, D. M., & Levy, B. I. (2013). Postischemic revascularization: From cellular and molecular mechanisms to clinical applications. *Physiological Reviews, 93*(4), 1743–1802.
6. Latremouille, C., Carpentier, A., Leprince, P., Roussel, J. C., Cholley, B., Boissier, E., et al. (2018). A bioprosthetic total artificial heart for end-stage heart failure: Results from a pilot study. *The Journal of Heart and Lung Transplantation, 37*(1), 33–37.
7. Smadja, D. M., Saubamea, B., Susen, S., Kindo, M., Bruneval, P., Van Belle, E., et al. (2017). Bioprosthetic Total artificial heart induces a profile of acquired Hemocompatibility with membranes Recellularization. *Journal of the American College of Cardiology, 70*(3), 404–406.
8. Debuc, B., & Smadja, D. M. (2020). (2020). Is COVID-19 a new hematologic disease? *Stem Cell Reviews and Reports, 12*, 1–5. https://doi.org/10.1007/s12015-020-09987-4.
9. Varga, Z., Flammer, A. J., Steiger, P., Haberecker, M., Andermatt, R., Zinkernagel, A. S., et al. (2020). Endothelial cell infection and endotheliitis in COVID-19. *Lancet*, 20.
10. Smadja, D.M., Guerin, C.L., Chocron, R., Yatim, N., Boussier, J., Gendron, N., et al. (2020). Angiopoietin-2 as a marker of endothelial activation is a good predictor factor for intensive care unit admission of COVID-19 patients. *Angiogenesis*, In press.
11. Ackermann, M., Verleden, S. E., Kuehnel, M., Haverich, A., Welte, T., Laenger, F., et al. (2020). Pulmonary vascular endothelialitis, thrombosis, and angiogenesis in Covid-19. *The New England Journal of Medicine, 383*(2), 120–128.
12. Khider, L., Gendron, N., Goudot, G., Chocron, R., Hauw-Berlemont, C., Cheng, C., et al. (2020). Curative anticoagulation prevents endothelial lesion in COVID-19 patients. *Journal of Thrombosis and Haemostasis*. https://doi.org/10.1111/jth.14968.
13. Wierz, M., Pierson, S., Guyonnet, L., Viry, E., Lequeux, A., Oudin, A., et al. (2018). Dual PD1/LAG3 immune checkpoint blockade limits tumor development in a murine model of chronic lymphocytic leukemia. *Blood, 131*(14), 1617–1621.
14. Qiu, P., Simonds, E. F., Bendall, S. C., Gibbs Jr., K. D., Bruggner, R. V., Linderman, M. D., Sachs, K., Nolan, G. P., & Plevritis, S. K. (2011). Extracting a cellular hierarchy from high-dimensional cytometry data with SPADE. *Nature Biotechnology, 29*(10), 886–891.
15. Becht, E., McInnes, L., Healy, J., Dutertre, C. A., Kwok, I. W. H., Ng, L. G., et al. (2019). Dimensionality reduction for visualizing single-cell data using UMAP. *Nature Biotechnology*.
16. Smadja, D. M., Mauge, L., Nunes, H., d'Audigier, C., Juvin, K., Borie, R., et al. (2013). Imbalance of circulating endothelial cells and progenitors in idiopathic pulmonary fibrosis. *Angiogenesis, 16*(1), 147–157.
17. Mauge, L., Sabatier, F., Boutouyrie, P., D'Audigier, C., Peyrard, S., Bozec, E., Blanchard, A., Azizi, M., Dizier, B., Dignat-George, F., Gaussem, P., & Smadja, D. M. (2014). Forearm ischemia decreases endothelial colony-forming cell angiogenic potential. *Cytotherapy, 16*(2), 213–224.
18. Smadja, D. M., Melero-Martin, J. M., Eikenboom, J., Bowman, M., Sabatier, F., & Randi, A. M. (2019). Standardization of methods to quantify and culture endothelial colony-forming cells derived from peripheral blood: Position paper from the International Society on Thrombosis and Haemostasis SSC. *Journal of Thrombosis and Haemostasis, 17*(7), 1190–1194.
19. Rigato, M., Avogaro, A., & Fadini, G. P. (2016). Levels of circulating progenitor cells, cardiovascular outcomes and death: A meta-analysis of prospective observational studies. *Circulation Research, 118*(12), 1930–1939.
20. Li, T. S., Hamano, K., Nishida, M., Hayashi, M., Ito, H., Mikamo, A., Matsuzaki, M., et al. (2003). CD117+ stem cells play a key role in therapeutic angiogenesis induced by bone marrow cell implantation. *American Journal of Physiology. Heart and Circulatory Physiology, 285*(3), H931–H937.
21. Cardenas, C., Kwon, J. Y., & Maeng, Y. S. (2016). Human cord blood-derived CD133(+)/C-kit(+)/Lin(−) cells have Bipotential ability to differentiate into Mesenchymal stem cells and outgrowth endothelial cells. *Stem Cells International, 2016*, 7162160.
22. Dhont, S., Derom, E., Van Braeckel, E., Depuydt, P., & Lambrecht, B. N. (2020). The pathophysiology of 'happy' hypoxemia in COVID-19. *Respiratory Research, 21*(1), 198.
23. Diehl, J. L., Peron, N., Chocron, R., Debuc, B., Guerot, E., Hauw-Berlemont, C., et al. (2020). Respiratory mechanics and gas exchanges in the early course of COVID-19 ARDS: A hypothesis-generating study. *Annals of Intensive Care, 10*(1), 95.
24. Billoir, P., Blandinieres, A., Gendron, N., Chocron, R., Gunther, S., Philippe, A., et al. (2020). Endothelial colony-forming cells from idiopathic pulmonary fibrosis patients have a high procoagulant potential. *Stem Cell Reports*. https://doi.org/10.1007/s12015-020-10043-4.
25. Ziegler, B. L., Valtieri, M., Porada, G. A., De Maria, R., Muller, R., Masella, B., et al. (1999). KDR receptor: A key marker defining hematopoietic stem cells. *Science, 285*(5433), 1553–1558.
26. Cosette, J., Moussy, A., Paldi, A., & Stockholm, D. (2017). Combination of imaging flow cytometry and time-lapse microscopy for the study of label-free morphology dynamics of hematopoietic cells. *Cytometry. Part A*, 91(3), 254–260.
27. Bendall, S. C., Davis, K. L., Amir el, A. D., Tadmor, M. D., Simonds, E. F., Chen, T. J., et al. (2014). Single-cell trajectory detection uncovers progression and regulatory coordination in human B cell development. *Cell, 157*(3), 714–725.
28. Zouggari, Y., Ait-Oufella, H., Bonnin, P., Simon, T., Sage, A. P., Guerin, C., et al. (2003). B lymphocytes trigger monocyte mobilization and impair heart function after acute myocardial infarction. *Nature Medicine, 19*(10), 1273–1280.
29. Werner, N., Kosiol, S., Schiegl, T., Ahlers, P., Walenta, K., Link, A., et al. (2005). Circulating endothelial progenitor cells and cardiovascular outcomes. *The New England Journal of Medicine, 353*(10), 999–1007.
30. Lu, R., Zhao, X., Li, J., Niu, P., Yang, B., Wu, H., et al. (2020). Genomic characterisation and epidemiology of 2019 novel

coronavirus: Implications for virus origins and receptor binding. *Lancet, 395*(10224), 565–574.
31. Quinti, I., Lougaris, V., Milito, C., Cinetto, F., Pecoraro, A., Mezzaroma, I., et al. (2020). A possible role for B cells in COVID-19?: Lesson from patients with Agammaglobulinemia. *The Journal of Allergy and Clinical Immunology*, 22.
32. Stanczuk, L., Martinez-Corral, I., Ulvmar, M. H., Zhang, Y., Lavina, B., Fruttiger, M., et al. (2017). cKit lineage hemogenic endothelium-derived cells contribute to mesenteric lymphatic vessels. *Cell Reports*.



## Affiliations

**Coralie L. Guerin[1,2,3] · Léa Guyonnet[1,2,3] · Guillaume Goudot[4] · Dominique Revets[3] · Maria Konstantinou[3] · Anna Chipont[3] · Richard Chocron[5,6] · Adeline Blandinieres[1,7] · Lina Khider[4] · Jeanne Rancic[1,8] · Christophe Peronino[1,7] · Benjamin Debuc[1,9] · Audrey Cras[1,10] · Camille Knosp[5] · Christian Latremouille[1,11] · Antoine Capel[12] · Markus Ollert[3] · Jean-Luc Diehl[1,8,13] · Piet Jansen[12] · Benjamin Planquette[1,8,14] · Olivier Sanchez[1,8,14] · Pascale Gaussem[1,15] · Tristan Mirault[5,16] · Alain Carpentier[1,11] · Nicolas Gendron[1,7] · David M. Smadja[1,7,17]**

1 Innovative Therapies in Haemostasis, INSERM, Université de Paris, F-75006 Paris, France
2 Cytometry Platform, Institut Curie, F-75006 Paris, France
3 Department of Infection and Immunity, Luxembourg Institute of Health, Strassen, Luxembourg
4 Vascular Medicine Department and Biosurgical Research Laboratory (Carpentier Foundation), AH-HP, Georges Pompidou European Hospital, Université de Paris, F-75015 Paris, France
5 PARCC, INSERM, Université de Paris, F-75006 Paris, France
6 Emergency Department, AH-HP, Georges Pompidou European Hospital, F-75015 Paris, France
7 Hematology Department and Biosurgical Research Laboratory (Carpentier Foundation), AH-HP, Georges Pompidou European Hospital, F-75015 Paris, France
8 Biosurgical Research Laboratory (Carpentier Foundation), AH-HP, Georges Pompidou European Hospital, F-75015 Paris, France
9 Plastic Surgery Department, AH-HP, Georges Pompidou European Hospital, F-75015 Paris, France
10 Cell therapy Unit, AP-HP, Saint Louis Hospital, F-75010 Paris, France
11 Cardiovascular Surgery Department and Biosurgical Research Laboratory (Carpentier Foundation) AP-HP, Georges Pompidou European Hospital, F-75015 Paris, France
12 Carmat SA, Vélizy-Villacoublay, France
13 Intensive Care Department and Biosurgical Research Laboratory (Carpentier Foundation), AH-HP, Georges Pompidou European Hospital, F-75015 Paris, France
14 Respiratory Medicine department and Biosurgical Research Laboratory (Carpentier Foundation), AH-HP, Georges Pompidou European Hospital, F-75015 Paris, France
15 Hematology Department, AH-HP, Georges Pompidou European Hospital, F-75015 Paris, France
16 Vascular Medicine department, AH-HP, Georges Pompidou European Hospital, F-75015 Paris, France
17 European Hospital Georges Pompidou, Inserm UMR-S 1140, 20 rue Leblanc, 75015 Paris, France